Electronic Research Archive

https://www.aimspress.com/journal/era

ERA, 33(12): 7699–7716.
DOI: 10.3934/era.2025340
Received: 04 November 2025
Revised: 06 December 2025
Accepted: 15 December 2025
Published: 22 December 2025

Research article

Finite-time formation control for multi-agent systems with dynamic leader and input saturation

Wenjie Li[1], **Xiangyong Chen**[1,2], **Ling Ji**[3,*], **Jinming Song**[1] and **Shuo Li**[1]

[1] School of Automation and Electrical Engineering, Linyi University, Linyi 276005, China
[2] School of Control Science and Engineering, Dalian University of Technology, Dalian 116024, China
[3] School of Logistics, Linyi University, Linyi 276005, China

* **Correspondence:** Email: jiling@lyu.edu.cn.

Abstract: In this paper, the problem of finite-time control for a group of quadrotor aircraft with an unknown input-saturation structure is investigated. Based on backstepping design, finite-time formation control algorithm is designed. Within the multi-agent systems, leaders are tasked with achieving formation consensus with an external leader. Concurrently, for the followers, a leader-follower consensus controller incorporating the dynamic leader's input is developed utilizing adaptive strategies and low-gain techniques. Thus, a hierarchical formation is achieved where leaders track the exogenous leader, followers maintain consensus with their leaders, accomplishing complex multi-unmanned aerial vehicle formation tasks.

Keywords: finite-time control; adaptive control; consensus tracking; dynamic leader; multi-agent systems; input saturation

1. Introduction

In recent years, the formation control of unmanned aerial vehicles (UAVs) has attracted significant research interest, driven by their extensive applicability in both civilian and military domains. In mission-critical environments, it is often imperative to establish a hierarchical architecture where leader UAVs maintain a formation relative to an exogenous leader, while follower UAVs track these leaders to facilitate distributed task execution. Prominent applications include cooperative aerial transport of heavy payloads, which resquires collaborative load distribution, and coordinated strikes against high-value targets, which require redundancy for effective saturation attacks. From a control-theoretic perspective, such systems impose substantial challenges.

Up to now, most existing results on formation control for a group of quadrotor aircraft have concern for asymptotic stability. From the viewpoint of convergence rate, it is desirable for the quadrotors to converge as rapidly as possible. In this context, the finite-time control technique introduced in [1], Bhat and Bernstein lay the theoretical groundwork for continuous finite-time stabilization. Furthermore, sources [2–4], applied terminal sliding mode control and continuous finite-time controller to rigid robots, demonstrating its finite-time convergence. In [5], a composite strategy with an observer is proposed to achieve rejection of perturbations. However, finite-time formation control for multi-agent systems(MASs) remains underexplored, as the inherent high dimensionality and strong nonlinear coupling significantly complicate controller synthesis and stability analysis.

The consensus tracking problem has been extensively explored in diverse scenarios. For instance, [6, 7] examined asymptotic consensus in heterogeneous MASs with unknown gains. Furthermore, considering practical constraints, [8] addressed the consensus tracking for multiple UAVs subject to distinct unknown time-varying delays, while [9] proposed a distributed observer-based approach to mitigate external disturbances and measurement sensor noise. A common limitation in these works, however, is the premise of an autonomous leader with zero control input. This assumption often fails to hold in practical applications, such as cooperative tracking of maneuvering targets where leader inputs are inherently nonzero and time-varying. Therefore, addressing consensus tracking for MASs that is subject to active leader inputs is imperative.

Input saturation constitutes a ubiquitous constraint in physical control systems, stemming inevitably from the finite capacity of the controller. Consequently, the consensus problem for MASs subject to saturation has been extensively investigated [10–14]. Among the proposed methodologies, low-gain feedback has emerged as a predominant strategy for preserving stability under constraints [15–18]. Alternatively, [19] employed anti-windup compensation to counteract saturation effects, provided that specific convexity conditions are met. Despite these advancements, the formation control problem for MASs which is simultaneously subject to input saturation and unknown, nonzero leader inputs remains an open challenge.

This work investigates formation consensus tracking for linear MASs subject to dynamic leadership and input saturation. The core challenge lies in achieving finite-time formation for dynamic leaders under controller saturation constraints. The primary contributions are summarized as follows:

- Distinguished from the asymptotically stable formation protocols studied in [20–23], the distributed formation control strategy proposed in this paper guarantees that cluster leaders achieve formation consensus with the exogenous leader in a finite time.
- This study broadens the scope of consensus tracking by addressing the challenging scenario of dynamic leaders with nonzero and unknown control inputs. Unlike standard approaches that rely on the restrictive assumption of a pre-determined trajectory leader, we introduce a robust adaptive compensation mechanism to reject the influence of the leader's maneuvering dynamics.
- Relative to [24–26], this paper ensures that control commands remain within feasible bounds while maintaining system stability, thereby bridging the gap between theoretical formation control and practical engineering implementation.

The remainder of this paper is organized as follows. Section 2 introduces preliminaries and the quadrotor model. Section 3 presents the design of the finite-time formation controller. In Section 4, two adaptive consensus tracking protocols are proposed. Section 5 provides a simulation example of finite-time formation control for a group of quadrotor aircraft. Finally, Section 6 concludes the paper.
Notations: Throughout this paper, $\mathfrak{R}^n$ and $\mathfrak{R}^{n\times n}$ refer to the real vector space of dimension n and the space of $n \times n$ real matrices, respectively. $|\cdot|$ denotes the absolute value and $||\cdot||$ the Euclidean norm of a

vector, the notation $\otimes$ is used for the Kronecker product, and abs$(\cdot)$ implies the absolute values of matrix entries. $\mathbf{1}_N$ stands for the $N \times 1$ vector with all elements being 1, and diag$\{\cdot\}$ signifies a diagonal matrix. $\lambda_{min}(\tilde{M})$ and $\lambda_{max}(\tilde{M})$ represent the minimal and maximal eigenvalues of matrix $\tilde{M}$, $tr(X)$ represents the trace of a square matrix X respectively.

2. Graph theory and model formulation

2.1. Graph theory

This work employs an undirected graph model to characterize the communication topology of a linear MAS. The graph is defined as $G = (\mathcal{V}, \mathcal{E}, \mathcal{A})$, where the node set $\mathcal{V} = \{1, \ldots, N\}$ comprises all agents in the system, the edge set $\mathcal{E} = \mathcal{V} \times \mathcal{V} = \{(i, j) : i, j \in \mathcal{V}\}$ describes connectivity between nodes, and the adjacency matrix is $\mathcal{A} = [a_{ij}] \in \mathbb{R}^{N\times N}$. If $(i, j) \in \mathcal{E}$, the $a_{ij} = 1$ otherwise, $a_{ij} = a_{ji} = 0$. The Laplacian matrix $\mathcal{L} = [l_{ij}] \in \mathbb{R}^{N\times N}$ is shown as $l_{ii} = \sum_{j=1,i\neq j}^{N} a_{ij}, l_{ij} = -a_{ij}$. The overall undirected topology G decomposes into M disjoint subgraphs $G_s = (\mathcal{V}_s, \mathcal{E}_s, \mathcal{A}_s)$ for $s \in (1, 2, \ldots, M)$, each representing a cluster within a hierarchical communication framework. The node set $\mathcal{V}$ partitions into non-empty subsets $\{\mathcal{V}_1, \mathcal{V}_2, \ldots, \mathcal{V}_M\}$. Each cluster contains exactly one designated leader node while remaining agents serve as followers. Intra-cluster communication is restricted to adjacent followers, whereas inter-cluster communication is exclusively managed by leaders.

The undirected graph $\bar{\mathcal{G}}_{M+1}$ with its Laplacian matrix $\mathcal{L}_{\bar{\mathcal{G}}_{M+1}}$ is used to denote the interaction among M leaders and the exogenous leader. The system additionally incorporates an exogenous leader l_0 with unknown inputs. The communication between leaders and the exogenous dynamic leader for the M leaders is defined as b_i. Specifically, $b_i = 1$ if the i-th leader receives information from the exogenous dynamic leader; otherwise, $b_i = 0$. Consequently, the leader adjacency matrix is given by $B_c = diag\{b_1, \cdots, b_n\}$, culminating in the augmented Laplacian $\bar{\mathcal{L}}_{\bar{\mathcal{G}}_{M+1}} = \mathcal{L}_{\bar{\mathcal{G}}_{M+1}} + B_c$. As same as above, the Laplacian matrix consisting of all followers within the subgraph $\mathcal{G}_s$ is defined as $\mathcal{L}_{\mathcal{G}_s}$. A leader adjacency matrix is defined for each cluster $\mathcal{G}_s$ by B_s. Then, its corresponding augmented Laplacian matrix is $\overline{\mathcal{L}}_{\mathcal{G}_s} = \mathcal{L}_{\mathcal{G}_s} + B_s$.

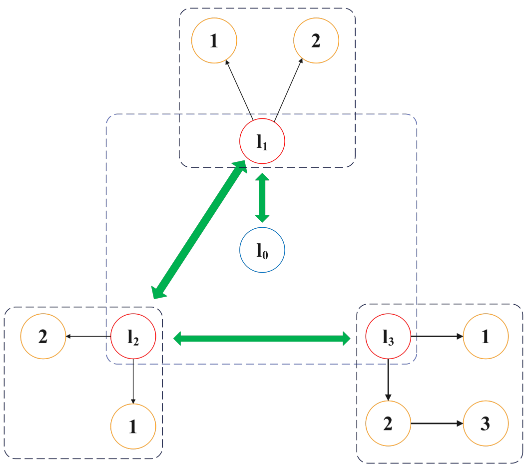

Figure 1. Clustered network.

Figure 1 illustrates a representative configuration comprising three clusters and one exogenous dynamic leader, where yellow, red, and blue nodes denote followers, cluster leaders, and the exogenous leader, respectively. Figure 2 illustrates a common formation pattern between the exogenous leader and the cluster leaders.

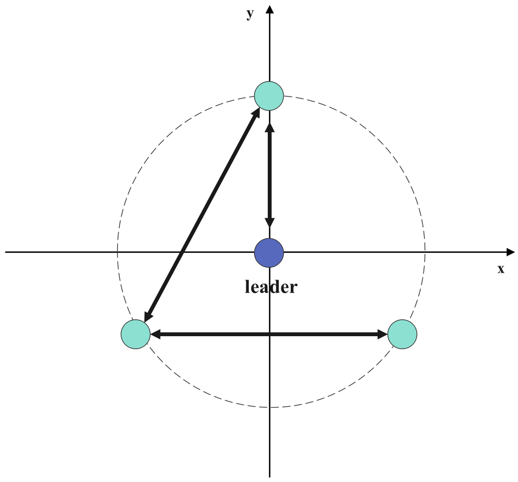

Figure 2. The communication topology graph and the formation pattern.

Assumption 2.1. *The communication topology among the M leaders is connected, and there exists at least one directed path from the leader to the external leader.*

2.2. System model

This paper investigates the formation control problem for leaders and the exogenous leader and the velocity consensus problem for leaders and followers. The position of the aircraft's center of mass relative to the inertial coordinate system is represented by $(x_{\tilde{i}}, y_{\tilde{i}}, z_{\tilde{i}})^T \in \mathbb{R}^3, \tilde{i} \in (l_1, \ldots, l_M, 1, \ldots, N)$. By accounting for external aerodynamic effects, the position dynamics of each quadrotor aircraft can be described by the following equations:

$$\begin{bmatrix} \ddot{x}_{\tilde{i}} \\ \ddot{y}_{\tilde{i}} \\ \ddot{z}_{\tilde{i}} \end{bmatrix} = -\frac{K_{\tilde{i}}}{m_{\tilde{i}}} \begin{bmatrix} \dot{x}_{\tilde{i}} \\ \dot{y}_{\tilde{i}} \\ \dot{z}_{\tilde{i}} \end{bmatrix} + \begin{bmatrix} \frac{T_{\tilde{i}}}{m_{\tilde{i}}}(\cos\phi_{\tilde{i}} \sin\theta_{\tilde{i}} \cos\psi_{\tilde{i}} + \sin\phi_{\tilde{i}} \sin\psi_{\tilde{i}}) \\ \frac{T_{\tilde{i}}}{m_{\tilde{i}}}(\cos\phi_{\tilde{i}} \sin\theta_{\tilde{i}} \sin\psi_{\tilde{i}} - \sin\phi_{\tilde{i}} \cos\psi_{\tilde{i}}) \\ \frac{T_{\tilde{i}}}{m_{\tilde{i}}} \cos\phi_{\tilde{i}} \cos\theta_{\tilde{i}} - g \end{bmatrix}. \tag{2.1}$$

In the dynamical model, the parameter m_i corresponds to the aircraft mass, the g represents the constant gravitational acceleration, the terms $K_{\tilde{i}} \in \mathbb{R}^+$ quantify the aerodynamic damping characteristics, and $\phi_{\tilde{i}}, \theta_{\tilde{i}}, \psi_{\tilde{i}}$ represents the three Euler angles.

2.3. Control objectives

The desired geometric configuration in three-dimensional space is specified by vectors $\Delta_{ij} \in \mathbb{R}^3$ for $i, j \in (l_1, \ldots, l_M)$ where $\Delta_{ij} = \Delta_i - \Delta_j = [\Delta_{i,x}, \Delta_{i,y}, \Delta_{i,z}]^T - [\Delta_{j,x}, \Delta_{j,y}, \Delta_{j,z}]^T$. One of the objectives is to devise a distributed control law to achieve finite-time formation control between the leaders and an exogenous leader. The finite-time formation requirements stipulate that both the desired formation pattern and the prescribed formation trajectory must be attained within a finite time T^* such that for any

$i, j \in (l_1, \ldots, l_M)$

$$\lim_{t \to T^*} \begin{bmatrix} x_i(t) - x_j(t) \\ y_i(t) - y_j(t) \\ z_i(t) - z_j(t) \end{bmatrix} \equiv \Delta_{ij}, \quad \forall t \geq T^*, \tag{2.2}$$

and

$$\lim_{t \to T^*} \frac{1}{m} \sum_{i=1}^{m} [x_i(t), y_i(t), z_i(t)]^T \equiv (x^d, y^d, z^d)^T, \quad \forall t \geq T^*. \tag{2.3}$$

Another objective of this paper is to design a controller $u_f(t)$ for followers $f \in (1, \ldots, N)$ that ensures their states track the leader's state, satisfying the condition

$$\lim_{t \to \infty} \|x_f(t) - x_l(t)\| \leq h, \tag{2.4}$$

where h is an arbitrary positive constant, x_l is the leader's position of the corresponding cluster. The realizability of these control objectives is guaranteed by the following assumptions and lemmas.

2.4. Related definitions and lemmas

This subsection introduces essential definitions and lemmas.

Definition 2.1. *Define a saturation function as follows*

$$\text{sat}_\alpha(x) = \begin{cases} \text{sign}(x), & \textit{for } |x| > 1, \\ \text{sig}^\alpha(x), & \textit{for } |x| \leq 1, \end{cases} \tag{2.5}$$

where $\alpha > 0$, $x \in \mathbb{R}$ and the function $\text{sig}^\alpha(x) = \text{sign}(x)|x|^\alpha$, $\text{sign}(\cdot)$ *denotes the standard signum function. For followers $f \in (1, \ldots, N)$, $sat(u_f) = sign(u_f) min(|u_f|, \Upsilon)$ where $\Upsilon > 0$ is the input saturation threshold for all followers.*

Definition 2.2. *[27] Consider a system described by $\dot{x} = f(x)$, where $f : U_0 \to \mathbb{R}^n$ is a continuous vector field defined on an open neighborhood U_0 of the origin, with $f(0) = 0$. Let $R = (r_1, r_2, \ldots, r_n)$ and a dilation tuple with $r_{\hat{q}} > 0$ for $\hat{q} = 1, \ldots, n$. The vector field $f(x) = (f_1(x), \ldots, f_n(x))^\top$ is said to be* homogeneous of degree *k with respect to the dilation R if for any $\varepsilon > 0$ and each component $f_{\hat{q}}$, the following scaling relation holds: $f_{\hat{q}}(\varepsilon^{r_1} x_1, \varepsilon^{r_2} x_2, \ldots, \varepsilon^{r_n} x_n) = \varepsilon^{k + r_{\hat{q}}} f_{\hat{q}}(x_1, x_2, \ldots, x_n)$, where the degree k satisfies $k > -\min\{r_1, r_2, \ldots, r_n\}$.*

Lemma 2.1. *[28] Consider the system $\dot{x} = f(x) + g(x), \quad x \in \mathbb{R}^m$, where $f(x)$ is a continuous homogeneous vector field of degree $k < 0$ with respect to the dilation $(r_1, \cdots, r_n)$, and $\hat{f}(x)$ satisfies $\hat{f}(0) = 0$. Suppose $x = 0$ is an asymptotically stable equilibrium of the nominal system $\dot{x} = f(x)$, and for all $x \neq 0$, the perturbation term $g(x)$ satisfies the limit condition:*

$$\frac{g_{\hat{p}}(\varepsilon^{r_1} x_1, \cdots, \varepsilon^{r_m} x_m)}{\varepsilon^{r_{\hat{p}} + k}} = 0, \quad \hat{p} = 1, 2, \cdots, n. \tag{2.6}$$

Then $x = 0$ is locally finite-time stable for the perturbed system. If the system is globally asymptotically stable in addition to being locally finite-time stable, then it is globally finite-time stable.

Lemma 2.2. *[29] Under Assumption 2.1, for each non-singular M-matrix* $\bar{\mathcal{L}}_{\mathcal{G}_{\hat{q}}}$ *with* $\hat{q} = 1, \ldots, M+1$, *there exists a positive definite diagonal matrix* $W_{\hat{q}} > 0$ *such that* $W_{\hat{q}}\bar{\mathcal{L}}_{\mathcal{G}_{\hat{q}}} + \bar{\mathcal{L}}_{\mathcal{G}_{\hat{q}}}^T W_{\hat{q}} > 0$. *Specifically, for* $\hat{q} = 1, \ldots, M$, *the weighting matrix is given by* $W_{\hat{q}} = \mathrm{diag}\{w_{s_{\hat{q}-1}+1}, \ldots, w_{s_{\hat{q}-1}+N_{\hat{q}}}\}$ *and* $[w_{s_{q-1}+1}, \ldots, w_{s_{\hat{q}-1}+N_{\hat{q}}}]^T = (\bar{\mathcal{L}}_{\mathcal{G}_{\hat{q}}}^T)^{-1}\mathbf{1}_{N_{\hat{q}}}$.

Lemma 2.3. *[30] Assume the pair* (A, B) *is stabilizable and matrix A has no eigenvalues in the open right-half plane. Then for any* $\iota \in (0, 1]$ *and constant* $\zeta > 0$, *there exists a unique positive definite solution* $Q > 0$ *to the algebraic Riccati equation* $A^T Q + QA - \zeta QBB^T Q + \iota I_n = \mathbf{0}_{n\times n}$. *Furthermore, this solution satisfies* $\lim_{\varepsilon\to 0^+} Q = \mathbf{0}_{n\times n}$.

Lemma 2.4. *[31] Let* $Z(t)$ *be a real function which satisfies the differential inequality* $\dot{Z}(t) \le -\tilde{p}Z(t) + \tilde{q}$ *for all* $t \ge 0$, *with constants* $\tilde{p} > 0$ *and* $\tilde{q} > 0$. *Then the following bound holds:* $Z(t) \le \left(Z(0) - \frac{\tilde{q}}{\tilde{p}}\right)e^{-\tilde{p}t} + \frac{\tilde{q}}{\tilde{p}}, \forall t \ge 0$.

3. Finite-time formation controller design

This section proposes the finite-time formation control algorithm, which includes two steps.

3.1. Controller design

For the purpose of designing the controller, let the dynamical equation be denoted as:

$$\begin{bmatrix} u_{i,x} \\ u_{i,y} \\ u_{i,z} \end{bmatrix} = \frac{T_i}{m_i}\begin{bmatrix} \cos\phi_i \sin\theta_i \cos\psi_i + \sin\phi_i \sin\psi_i \\ \cos\phi_i \sin\theta_i \sin\psi_i - \sin\phi_i \cos\psi_i \\ \cos\phi_i \cos\theta_i \end{bmatrix} - \begin{bmatrix} 0 \\ 0 \\ g \end{bmatrix}. \tag{3.1}$$

Using this notation, the position dynamics of the i-th quadrotor can be reformulated as:

$$\begin{bmatrix} \ddot{x}_i \\ \ddot{y}_i \\ \ddot{z}_i \end{bmatrix} = -\frac{K_i}{m_i}\begin{bmatrix} \dot{x}_i \\ \dot{y}_i \\ \dot{z}_i \end{bmatrix} + \begin{bmatrix} u_{i,x} \\ u_{i,y} \\ u_{i,z} \end{bmatrix} \tag{3.2}$$

Theorem 3.1. *For the position dynamic model* (3.2), *if the virtual control inputs are designed as follows:*

$$\begin{aligned} u_{i,p^*} = &-\sum_{j\in N_i} a_{ij}\Big[k_1 \mathrm{sat}_{\alpha_1}(p_i^* - p_j^* - \Delta_{ij,p^*}) + k_2 \mathrm{sat}_{\alpha_2}(v_{i,p^*} - v_{j,p^*})\Big] \\ &- b_i\Big[k_1 \mathrm{sat}_{\alpha_1}\left(p_i^* - p^{*d} - \Delta_{i,p^*} + \frac{1}{M}\sum_{i=1}^{M}\Delta_{i,p^*}\right) + k_2 \mathrm{sat}_{\alpha_2}(v_{i,p^*} - v_{p^*}^d)\Big] \\ &+ \frac{K_i}{m_i}v_{p^*}^d + \dot{v}_{p^*}^d, \end{aligned} \tag{3.3}$$

where $\dot{x}^d = v_x^d, \dot{y}^d = v_y^d, \dot{z}^d = v_z^d$, *and* p^* *denote the position component along the three coordinate axes (x, y, z). The set of neighbors of node i is denoted by* $N_i = \{j : (v_i, v_j) \in \mathcal{V}\}$. *The formation control objective is achieved within a finite time under the conditions that* $k_1 > 0$, $k_2 > 0$, $0 < \alpha_1 < 1$, *and* $\alpha_2 = 2\alpha_1/(1 + \alpha_1)$.

Proof. Without loss of generality, the proof focuses on the x-axis dynamics. Accordingly, the coordinate transformation for the i-th quadrotor is defined as

$$e_{i,xp} = x_i - \Delta_{i,x} - x^d + \frac{\sum_{i=1}^{n} \Delta_{i,x}}{n}, e_{i,xv} = v_{i,x} - v_x^d, i \in (l_1, \ldots, l_M) \tag{3.4}$$

The subsequent analysis will demonstrate that the multi-agent system (3.4) is globally finite-time stable, with the proof proceeding in two main steps.

The first step is to prove the asymptotic stability of the system. A candidate Lyapunov function for system (3.4) is constructed as

$$V = \sum_{i=1}^{M} \sum_{j=1}^{M} a_{ij} k_1 \int_0^{e_{i,xp} - e_{j,xp}} \mathrm{sat}_{\alpha_1}(\varepsilon) \mathrm{d}\varepsilon + \sum_{i=1}^{M} e_{i,xv}^2 + \sum_{i=1}^{M} \int_0^{e_{i,xp}} 2 b_i k_1 \mathrm{sat}_{\alpha_1}(\varepsilon) \mathrm{d}\varepsilon, \tag{3.5}$$

where $i, j \in (1, 2, ..., M)$, $j \neq i$. Given $0 < \alpha_1 < 1$, $V = 0$ if and only if the error vector $(e_{1,xp}, \cdots, e_{n,xp}) = 0$, thus $V \geq 0$. The time derivative of V along the trajectories of system (3.4) is given by

$$\begin{aligned}
\dot{V} &= -2 \sum_{i=1}^{M} e_{i,xv} \left(\sum_{j=1}^{M} a_{ij} [k_1 \mathrm{sat}_{\alpha_1}(\tilde{\Delta_p}) + k_2 \mathrm{sat}_{\alpha_2}(\tilde{\Delta_v})] + b_i [k_1 \mathrm{sat}_{\alpha_1}(e_{i,xp}) + k_2 \mathrm{sat}_{\alpha_2}(e_{i,xv})] + \frac{K_i}{m_i} e_{i,xv} \right) \\
&\quad + k_1 \sum_{i=1}^{M} \left(\sum_{j=1}^{M} a_{ij} \tilde{\Delta}_v \mathrm{sat}_{\alpha_1}(\tilde{\Delta_p}) + 2 b_i [\mathrm{sat}_{\alpha_1}(e_{i,xp})] e_{i,xv} \right) \\
&= - \sum_{i=1}^{M} \left(\sum_{j=1}^{M} a_{ij} \tilde{\Delta}_v [k_1 \mathrm{sat}_{\alpha_1}(\tilde{\Delta_p}) + k_2 \mathrm{sat}_{\alpha_2}(\tilde{\Delta}_v)] + 2 b_i e_{i,xv} [k_1 \mathrm{sat}_{\alpha_1}(e_{i,xp}) + k_2 \mathrm{sat}_{\alpha_2}(e_{i,xp})] \right) - 2 \sum_{i=1}^{M} \frac{K_i}{m_i} e_{i,xv}^2 \\
&\quad + k_1 \sum_{i=1}^{M} \left(\sum_{j=1}^{M} a_{ij} \tilde{\Delta}_v k_1 [\mathrm{sat}_{\alpha_1}(\tilde{\Delta_p})] + 2 b_i k_2 \mathrm{sat}_{\alpha_1}(e_{i,xp}) e_{i,xv} \right),
\end{aligned} \tag{3.6}$$

where $\tilde{\Delta_v} = e_{i,xv} - e_{j,xv}$, $\tilde{\Delta_p} = e_{i,xp} - e_{j,xp}$. The time derivative of V along the system (3.1) is obtained as

$$\dot{V} = -k_2 \sum_{i=1}^{M} \left(\sum_{j=1}^{M} a_{ij} \tilde{\Delta}_v \mathrm{sat}_{\alpha_2}(\tilde{\Delta}_v) + 2 b_i e_{i,xv} \mathrm{sat}_{\alpha_2}(e_{i,xv}) \right) - 2 \sum_{i=1}^{M} \frac{K_{i,1}}{m_i} e_{i,xv}^2, \tag{3.7}$$

where $a_{ij} \geq 0$, $b_i \geq 0$; then it can be concluded that $\dot{V} \leq 0$. Above all, the system (3.4) is globally asymptotically stable.

Building upon global asymptotic stability, the second step is to prove that the system achieves finite-time stability. Given the global asymptotic stability of the system (3.4), the states of the system $(e_{i,xp}, e_{i,xv})$ will converge to the region $\Omega = \left\{(e_{i,xp}, e_{i,xv}) : |e_{i,xp}| \leq 1, |e_{i,xv}| \leq 1, i \in (1, 2, ...M)\right\}$ within finite time and remain there. After then, the system (3.4) can be rewrite as

$$\dot{e}_{i,xp} = e_{i,xv}$$

$$\dot{e}_{i,xv} = -\sum_{j \in N_i} a_{ij} \left[k_1 \mathrm{sign}^{\alpha_1}(\tilde{\Delta_p}) + k_2 \mathrm{sign}^{\alpha_2}(\tilde{\Delta_v})\right] - b_i \left[k_1 \mathrm{sign}^{\alpha_1}(e_{i,xp}) + k_2 \mathrm{sign}^{\alpha_2}(e_{i,xv})\right] - g(e_{i,xv}), \tag{3.8}$$

where $g(e_{i,xv}) = K_i e_{i,xv}/m_i$. For any $(e_{i,xp}, e_{i,xv}) \neq 0$, we have

$$\lim_{\xi\to 0}\frac{(\xi^{r_2} e_{i,xv})}{\xi^{r_2+k}} = \lim_{\xi\to 0} -\frac{\frac{K_i}{m_i}\xi^{r_2} e_{i,xv}}{\xi^{r_2+k}} = \lim_{\xi\to 0} -\frac{K_i}{m_i}\xi^{-k} e_{i,xv} = 0. \tag{3.9}$$

Therefore, the linear damping term $g(e_{i,xv})$ is the perturbation that fulfills the criteria specified in Lemma 2.1. Choose the Lyapunov function as

$$\bar{V} = \sum_{i=1}^{M} e_{i,xv}^2 + \sum_{i=1}^{M}\sum_{j=1}^{M} a_{ij}k_1 \int_0^{\tilde{\Delta}_p} \mathrm{sig}^{\alpha_1}(\varepsilon)\mathrm{d}\varepsilon + 2k_1 \sum_{i=1}^{M} b_i \int_0^{e_{i,xp}} \mathrm{sig}^{\alpha_1}(\varepsilon)\mathrm{d}\varepsilon. \tag{3.10}$$

After excluding the linear damping term $g(e_{i,xv})$ based on the requirements of Lemma 2.1 the time derivative of $\bar{V}$ is

$$\dot{\bar{V}} = -k_2 \sum_{i=1}^{M}\sum_{j=1}^{M} a_{ij}\tilde{\Delta}_v \mathrm{sig}^{\alpha_2}(\tilde{\Delta}_v) - k_2 \sum_{i=1}^{M} 2b_i e_{i,xv}\mathrm{sig}^{\alpha_2}(e_{i,xv}) \leq 0. \tag{3.11}$$

According to Definition 2.2, system (3.8) can be verified to be homogeneous of degree $k = (\alpha_1 - 1)/2 < 0$ with respect to the dilation. Based on Lemma 2.1, system (3.8) is global finite-time stability. Thus, there exists a time T^* such that

$$\lim_{t\to T^*}(e_{i,xp}(t), e_{i,xv}(t)) \equiv 0, \quad t \geq T^*. \tag{3.12}$$

Based on the coordinate transformations defined in (3.4), it follows that for any $i, j \in (1, 2, \cdots, M)$ $\lim_{t\to T^*}[x_i(t) - x_j(t)] = \Delta_{i,x} - \Delta_{j,x} = \Delta_{ij,x}$, and $\lim_{t\to T^*} \frac{1}{n}\sum_{i=1}^{n} x_i(t) = x^d$. For $t \geq T^*$ $[x_i(t) - x_j(t)] = \Delta_{i,x} - \Delta_{j,x} \equiv \Delta_{ij,x}$. Therefore, the formation control objective between leaders and exogenous leader can be achieved within finite time. □

Remark 3.1. *It is worth noting that the proposed finite-time control strategy degenerates into a classical PD controller when the fractional power parameters are set to* $\alpha_1 = \alpha_2 = 1$. *To demonstrate the superiority of the finite-time technique, a comparative analysis of the system performance under both control schemes is presented in the simulation section.*

4. Consensus tracking analysis between leaders and followers

Under operational scenarios requiring redundant saturation attacks or heavy-load transportation, followers often share co-located initial positions with the leaders. Under such conditions, to reduce communication overhead and control effort, the follower's controller should be designed based primarily on its own velocity, enabling it to maintain velocity consistency with the leader even in the presence of exogenous acceleration inputs to the leader. Assuming the dynamics of follower is given by

$$\dot{v}_f(t) = Av_f(t) + B\,\mathrm{sat}(u_f), \tag{4.1}$$

define $e_{f,l} = v_f - v_l$ as the tracking error between the leader of the corresponding cluster and the followers. And the time derivative of $e_{f,l}$ is

$$\dot{e}_{f,l} = Ae_{f,l} + B\,\mathrm{sat}(u_f) - Bu_l, f \in \{1, ..., N\}. \tag{4.2}$$

We present the following distributed adaptive control law for follower F:

$$u_f = u_f^{TC} + u_f^{LI}, \tag{4.3}$$

where u_f^{TC} is the consensus tracking controller designed by ignoring the leader's input, and u_f^{LI} is the robust adaptive compensator introduced to restrain the influence of u_l. Specifically, u_f^{TC} is constructed as

$$\begin{aligned} u_f^{TC} &= \alpha_f K \eta_f \\ \dot{\alpha}_f &= (\Gamma_f^{-1})^T K e_{f,l} \eta_f^T K^T - \vartheta_f \alpha_f, \end{aligned} \tag{4.4}$$

where $\eta_f = \sum_{j=F_1}^{F_N} a_{fj}(v_f - v_j) + d_{f,l}(v_f - v_l)$, $\vartheta_f > 0$, $\alpha_f \in \mathbb{R}^{m\times m}$ represents the adaptive coupling weight with $\alpha_f(0) > 0$, $K = -B^T Q \in \mathbb{R}^{m\times n}$ is the control gain matrix, and $\Gamma_f \in \mathbb{R}^{m\times m} > 0$ adjusts the convergence rate of α_f. To deal with the unknown leader's input u_l, u_f^{LI} is designed as

$$\begin{aligned} u_f^{LI} &= \frac{\beta_f K e_{f,l}}{\chi_f + \|K e_{f,l}\|}, \\ \dot{\beta}_f &= \theta_f(1 - \beta_f) + \varrho_f \|K e_{f,l}\|, \end{aligned} \tag{4.5}$$

where $\beta_f(0) > 1$ represents the adaptive coupling weight and χ_f, θ_f, ϱ_f are nonnegative constants. Note that $\beta_f(0) \geq 1$ and $\dot{\beta}_f \geq 0$ when $\beta_f = 1$ in (4.5); it directly follows that $\beta_f(t) \geq 1$. According to Lemma 2.3, it is easy to see that $\lim_{\varepsilon\to 0^+} Q = \mathbf{0}_{n\times n}$ holds. Combing this with (4.3)–(4.5), we can choose an appropriate ι such that Q is sufficiently small, thereby satisfying the inequality as below:

$$\left\| u_f^{TC} + u_f^{LI} \right\| \leq \sqrt{m}\,\Upsilon. \tag{4.6}$$

Then, $\dot{e}_{f,l}$ can be rewritten as

$$\dot{e}_{f,l} = A e_{f,l} + B(\alpha_f K \eta_f + u_f^{LI} - u_l). \tag{4.7}$$

Theorem 4.1. *Suppose provided the Assumptions hold, the fully distributed control law (4.3)–(4.5) guarantees that the tracking errors $e_{f,l}$ and adaptive gains α_f,β_f ($f \in \mathcal{V}_f$) are UUB for the leader-follower subsystem.*

Proof. We choose the Lyapunov function candidate as

$$\tilde{V}_1 = \sum_{f=F_1}^{F_N} \left(\frac{w_f}{\varrho_f}\tilde{\beta}_f^2 + w_f e_{f,l}^T Q e_{f,l}\right) + tr\left(\sum_{f=F_1}^{F_N} w_f \tilde{\alpha}_f^T \Gamma_f \tilde{\alpha}_f\right), \tag{4.8}$$

where w_f is defined in Lemma 2.2, $\tilde{\alpha}_f = \alpha_f - \delta_1 I_m$, and $\tilde{\beta}_f = \beta_f - \delta_2$ with $\delta_1, \delta_2 > 0$. Taking the derivative of $\sum_{f=F_1}^{F_N} w_f e_{f,l}^T Q e_{f,l}$ in (4.8) along the trajectories of (4.7) yields

$$\begin{aligned}
2\sum_{f=F_1}^{F_N} w_f e_{f,l}^T Q \dot{e}_{f,l} &= 2\sum_{f=F_1}^{F_N} w_f e_{f,l}^T Q(Ae_{f,l} + Bu_f - Bu_l) \\
&= 2\sum_{f=F_1}^{l_N} w_f e_{f,l}^T QAe_{f,l} + 2\sum_{f=F_1}^{F_N} w_f e_{f,l}^T QBu_f - 2\sum_{f=F_1}^{F_N} w_f e_{f,l}^T QBu_l \\
&= -2e_l^T (W_{N+1}\mathbf{1}_N \otimes QB)\, u_l + 2e_l^T (W_{N+1} \otimes QA)\, e_l - 2\sum_{f=F_1}^{F_N} w_f e_{f,l}^T K^T (\alpha_f K\eta_f + u_f^{LI}) \\
&\leq e_l^T \left[W_{N+1} \otimes \left(QA + A^T Q \right) \right] e_l - 2\sum_{f=F_1}^{F_N} w_f e_{f,l}^T K^T (\alpha_f K\eta_f + u_f^{LI}) + 2\bar{u}_l \sum_{f=F_1}^{F_N} w_f \|Ke_{f,l}\|,
\end{aligned} \tag{4.9}$$

where $e_l = [e_{F_1,l}^T, \ldots, e_{F_N,l}^T]^T$. The derivative of $tr\left(\sum_{f=F_1}^{F_N} w_f \tilde{\alpha}_f^T \Gamma_f \tilde{\alpha}_f\right)$ can be computed as

$$\begin{aligned}
2tr\left(\sum_{f=F_1}^{F_N} w_f \dot{\tilde{\alpha}}_f^T \Gamma_f \tilde{\alpha}_f \right) &= 2tr\left(\sum_{f=F_1}^{F_N} w_f \dot{\tilde{\alpha}}_f^T \Gamma_f \alpha_f \right) - 2\delta_1 tr\left(\sum_{f=F_1}^{F_N} w_f \dot{\tilde{\alpha}}_f^T \Gamma_f \right) \\
= 2tr\left(\sum_{f=F_1}^{F_N} w_f \left(K\eta_f e_{f,l}^T K^T \alpha_f - \vartheta_f \alpha_f^T \Gamma_f \alpha_f \right) \right) &- 2\delta_1 tr\left(\sum_{f=F_1}^{F_N} w_f \left(K\eta_f e_{f,l}^T K^T - \vartheta_f \alpha_f^T \Gamma_f \right) \right).
\end{aligned} \tag{4.10}$$

Because $K^T K\eta_f = \Psi \sum_{j=F_1}^{F_N} [a_{fj}(e_{f,l} - e_{j,l}) + d_{f,l} e_{f,l}]$, one has

$$\begin{aligned}
&2tr\left(\sum_{f=F_1}^{F_N} w_f K\eta_f e_{f,l}^T K^T \alpha_f \right) - 2\delta_1 tr\left(\sum_{f=F_1}^{F_N} w_f K\eta_f e_{f,l}^T K^T \right) \\
&= 2\sum_{f=F_1}^{F_N} w_f e_{f,l}^T K^T \alpha_f K\eta_f - 2\delta_1 \sum_{f=F_1}^{F_N} w_f e_{f,l}^T \Psi \left[\sum_{j=F_1}^{F_N} a_{fj}(e_{f,l} - e_{j,l}) + d_{f,l} e_{f,l} \right] \\
&= 2\sum_{f=F_1}^{F_N} w_f e_{f,l}^T K^T \alpha_f K\eta_f - 2\delta_1 \sum_{f=F_1}^{F_N} \sum_{j=F_1}^{F_N} \bar{l}_{fj} w_f e_{f,l}^T \Psi e_{j,l},
\end{aligned} \tag{4.11}$$

where $\bar{l}_{fj}$ is the element of matrix $\bar{\mathcal{L}}_{\mathcal{G}_{M+1}}$, and $\Psi = QBB^T Q$. Because $-\tilde{\alpha}_f^T \Gamma_f \tilde{\alpha}_f = -\left(\alpha_f^T \Gamma_f \alpha_f - \alpha_f^T \Gamma_f \delta_1 - \delta_1 \Gamma_f \alpha_f + \delta_1^2 \Gamma_f \right)$, we have

$$- 2tr\left(\sum_{f=F_1}^{F_N} w_f \vartheta_f \alpha_f^T \Gamma_f (\alpha_f - \delta_1 I_m) \right) \leq -tr\left(\sum_{f=F_1}^{F_N} w_f \vartheta_f \tilde{\alpha}_f^T \Gamma_f \tilde{\alpha}_f \right) + \delta_1^2 tr\left(\sum_{f=F_1}^{F_N} w_f \vartheta_f \Gamma_f \right). \tag{4.12}$$

Substituting (4.11) and (4.12) into (4.10) yields:

$$\begin{aligned}
2tr\left(\sum_{f=F_1}^{F_N} w_f \dot{\tilde{\alpha}}_f^T \Gamma_f \tilde{\alpha}_f \right) \leq\ & 2\sum_{f=F_1}^{F_N} w_f e_{f,l}^T K^T \alpha_f K\eta_f - 2\delta_1 \sum_{f=F_1}^{F_N} \sum_{j=F_1}^{F_N} \bar{l}_{fj} w_f e_{f,l}^T \Psi e_{j,l} \\
& - tr\left(\sum_{f=F_1}^{F_N} w_f \vartheta_f \left(\tilde{\alpha}_f^T \Gamma_f \tilde{\alpha}_f - \delta_1^2 \Gamma_f \right) \right).
\end{aligned} \tag{4.13}$$

Taking the time derivative of $\sum_{f=F_1}^{F_N}\frac{w_f}{\varrho_f}\tilde{\beta}_f^2$, we obtain

$$\sum_{f=F_1}^{F_N}\frac{2w_f}{\varrho_f}\tilde{\beta}_f\dot{\beta}_f = 2\sum_{f=F_1}^{F_N} w_f(\beta_f-\delta_2)\|Ke_{f,l}\| - 2\sum_{f=F_1}^{F_N}\frac{w_f\theta_f}{\varrho_f}\tilde{\beta}_f\beta_f + 2\sum_{f=F_1}^{F_N}\frac{w_f\theta_f}{\varrho_f}\tilde{\beta}_f. \tag{4.14}$$

By using Young's inequality we have $-2\tilde{\beta}_f(\beta_f-1)\leq -\frac{1}{2}\tilde{\beta}_f^2-\frac{1}{2}(\beta_f-1)^2+(\delta_2-1)^2$. And $-2\sum_{f=F_1}^{F_N}\frac{w_f\theta_f}{\varrho_f}\tilde{\beta}_f\beta_f+2\sum_{f=F_1}^{F_N}\frac{w_f\theta_f}{\varrho_f}\tilde{\beta}_f=-2\sum_{f=F_1}^{F_N}\frac{w_f\theta_f}{\varrho_f}\tilde{\beta}_f(\beta_f-1)$, we can get

$$\begin{aligned}
-2\sum_{f=F_1}^{F_N}\frac{w_f\theta_f}{\varrho_f}\tilde{\beta}_f(\beta_f-1) &\leq -\sum_{f=F_1}^{F_N}\frac{w_f\theta_f}{2\varrho_f}\tilde{\beta}_f^2 + \sum_{f=F_1}^{F_N}\frac{w_f\theta_f}{\varrho_f}(\delta_2-1)^2 - \sum_{f=F_1}^{F_N}\frac{w_f\theta_f}{2\varrho_f}(\beta_f-1)^2 \\
&\leq -\sum_{f=F_1}^{F_N}\frac{w_f\theta_f}{\varrho_f}\left(\frac{1}{2}\tilde{\beta}_f^2+\frac{1}{4}\beta_f^2\right) + \sum_{f=F_1}^{F_N}\frac{w_f\theta_f}{\varrho_f}(\delta_2-1)^2 + \sum_{f=F_1}^{F_N}\frac{w_f\theta_f}{2\varrho_f}.
\end{aligned} \tag{4.15}$$

Substituting (4.9), (4.13), (4.14), and (4.15) yields the time derivative of $\tilde{V}_1$ as:

$$\begin{aligned}
\dot{\tilde{V}}_1 \leq & e_l^T\left[W_{N+1}\otimes\left(QA+A^TQ\right)\right]e_l - 2\sum_{f=F_1}^{F_N} w_f e_{f,l}^T K^T u_f^{LI} + 2\bar{u}_l\sum_{f=F_1}^{F_N} w_f\|Ke_{f,l}\| - \sum_{f=F_1}^{F_N}\frac{w_f\theta_f}{2\varrho_f}\tilde{\beta}_f^2 \\
& - 2\delta_1\sum_{f=F_1}^{F_N}\sum_{j=F_1}^{F_N}\bar{l}_{fj}w_f e_{f,l}^T\Psi e_{j,l} + 2\sum_{f=F_1}^{F_N} w_f\beta_f\|Ke_{f,l}\| - 2\delta_2\sum_{f=F_1}^{F_N} w_f\|Ke_{i,l}\| - \sum_{f=F_1}^{F_N}\frac{w_f\theta_f}{4\varrho_f}\beta_f^2 \\
& + \sum_{f=F_1}^{F_N}\frac{w_f\theta_f}{2\varrho_f} - tr\left(\sum_{f=F_1}^{F_N} w_f\vartheta_f\tilde{\alpha}_f^T\Gamma_f\tilde{\alpha}_f\right) + \delta_1^2 tr\left(\sum_{f=F_1}^{F_N} w_f\vartheta_f\Gamma_f\right) + \sum_{f=F_1}^{F_N}\frac{w_f\theta_f}{\varrho_f}(\delta_2-1)^2.
\end{aligned} \tag{4.16}$$

According to (4.5), one obtains

$$\begin{aligned}
& 2\sum_{f=F_1}^{F_N} w_f\beta_f\|Ke_{f,l}\| - 2\sum_{f=F_1}^{F_N} w_f e_{f,l}^T K^T u_f^{LI} - \sum_{f=F_1}^{F_N}\frac{w_f\theta_f}{4\varrho_f}\beta_f^2 \\
&= -2\sum_{f=F_1}^{F_N} w_f\beta_f(\|Ke_{f,l}\|+\chi_f) + 4\sum_{f=F_1}^{F_N} w_f\beta_f\frac{\|Ke_{f,l}\|\chi_f}{\|Ke_{f,l}\|+\chi_f} \\
&\quad + 2\sum_{f=F_1}^{F_N} w_f\beta_f\frac{\chi_f^2}{\|Ke_{f,l}\|+\chi_f} + 2\sum_{f=F_1}^{F_N} w_f\beta_f\|Ke_{f,l}\| - \sum_{f=F_1}^{F_N}\frac{w_f\theta_f}{4\varrho_f}\beta_f^2 \\
&\leq -\sum_{f=F_1}^{F_N} w_f\beta_f\left(\frac{\theta_f}{4\varrho_f}-4\chi_f\right).
\end{aligned} \tag{4.17}$$

Substituting (4.17) into (4.16) and setting $\delta_2>\bar{u}_l$, $\frac{\theta_f}{\varrho_f\chi_f}\geq 16$ and $\delta_1\geq\frac{2\bar{w}}{\lambda_{min}(W_{N+1},\mathcal{L}_{Q,N+1}+\mathcal{L}_{Q,N+1}^T}W_{N+1})$ yields

$$\dot{\tilde{V}}_1 \leq e_l^T\left[W_{N+1}\otimes\left(QA+A^TQ-2\Psi\right)\right]e_l - tr\left(\sum_{f=F_1}^{F_N} w_f\vartheta_f\tilde{\alpha}_f^T\Gamma_f\tilde{\alpha}_f\right) - \sum_{f=F_1}^{F_N}\frac{w_f\theta_f}{2\varrho_f}\tilde{\beta}_f^2 + \Delta, \tag{4.18}$$

where $\Delta = \delta_1^2 tr\left(\sum_{f=F_1}^{F_N} w_f\vartheta_f\Gamma_f\right) + \sum_{f=F_1}^{F_N} \frac{w_f\theta_f}{\varrho_f}[(\delta_2-1)^2+\frac{1}{2}]$ and $\overline{w} = max\{w_{F_1},\ldots,w_{F_N}\}$. Based on Lemma 2.3, we rewrite (4.18) into

$$\begin{aligned}\tilde{V}_1 \leq & -\iota e_l^T\left(W_{N+1}\otimes I_n\right)e_l - \sum_{f=F_1}^{F_N}\frac{w_f\theta_f}{2\varrho_f}\tilde{\beta}_f^2 - tr\left(\sum_{f=F_1}^{F_N} w_f\vartheta_f\tilde{\alpha}_f^T\Gamma_f\tilde{\alpha}_f\right)+\Delta \\ \leq & -\sum_{f=F_1}^{F_N}(\iota-\rho_1\lambda_{max}(Q))w_f e_{f,l}^T e_{f,l} - tr\left(\sum_{f=F_1}^{F_N}(\vartheta_f-\rho_1)w_f\tilde{\alpha}_f^T\Gamma_f\tilde{\alpha}_f\right) \\ & -\sum_{f=F_1}^{F_N}\left(\frac{\theta_f}{2}-\rho_1\right)\frac{w_f}{\varrho_f}\tilde{\beta}_f^2+\Delta-\rho_1 V_1,\end{aligned} \tag{4.19}$$

where $\rho_1 = min\{\frac{\varepsilon}{2\lambda_{max}(Q)}, \vartheta_f, \frac{\theta_f}{2}\}$. Based on this definition, we can conclude that

$$\tilde{V}_1 \leq -\frac{\iota\underline{w}}{2}||e_l||^2 - \rho_1\tilde{V}_1 + \Delta \leq -\rho_1\tilde{V}_1 + \Delta, \tag{4.20}$$

where $\underline{w} = min\{w_{F_1},\ldots,w_{F_N}\}$. In light of Lemma 2.4, we can deduce from (4.20) that $\tilde{V}_1$ exponentially converges to the residual set

$$\tilde{V}_1 \leq \frac{\Delta}{\rho_1} + \left(\tilde{V}_1(0) - \frac{\Delta}{\rho_1}\right)e^{-\rho_1 t}. \tag{4.21}$$

Let $\bar{\varrho} = max\{\varrho_{F_1},\ldots,\varrho_{F_N}\}$. Given the lower bound $\tilde{V}_1 \geq \underline{w}\lambda_{min}(Q)||e_l||^2 + \frac{\underline{w}}{\bar{\varrho}}\sum_{f=F_1}^{l_M}\tilde{\beta}_f^2 + \underline{w}tr\left(\sum_{f=F_1}^{F_N}\tilde{\alpha}_f^T\Gamma_f\tilde{\alpha}_f\right)$, implies that $e_{f,l}, \alpha_f$ and β_f are UUB. Moreover, whenever $||e_l||^2 \geq \frac{2}{\iota\underline{w}}\Delta$, the first inequality in (4.20) yields $\tilde{V}_1 \leq -\rho_1\tilde{V}_1$. Consequently, the tracking error e_l exhibits exponential convergence to the residual set $\mathcal{D} = \{e_l : ||e_l||^2 \leq \frac{2}{\iota\underline{w}}\Delta\}$ with a decay rate exceeding $e^{-\rho_1 t}$. □

Remark 4.1. *The proposed controller* (3.3) *incorporates the saturation constraint, thereby defining the bound for the controller as:*

$$(k_1+k_2)\left(\sum_{j\in N_i} a_{ij} + b_i\right) + \frac{K_{i,3}}{m_i}|v^d| + |\dot{v}^d|. \tag{4.22}$$

Furthermore, the followers controller satisfies $sat(u_f) = sign(u_f)min(|u_f|,\Upsilon)$. Consequently, the controllers for both the leader and the followers are bounded.

5. Numerical simulation

In this section, an example is provided to demonstrate the efficacy of the theoretical results given in the previous section. This example considers a hierarchical cluster network as shown in Figure 1. Specifically, the agent labeled l_0 is the exogenous dynamic leader; agents labeled l_1, l_2 and l_3 are the leaders of cluster 1, cluster 2 and cluster 3, respectively. The communication topology among the quadrotor aircraft is described by an undirected graph as depicted in Figure 2. The edge weights are assigned as follows: $a_{12} = a_{21} = 1$, $a_{23} = a_{32} = 1$, and $b_1 = 1$. A regular triangle formation in the X-Z plane is chosen as the desired formation pattern. The relative position deviations are specified as

$$\Delta_{12} = \Delta_1 - \Delta_2 = \left([0,0,1]^T - [\cos(5\pi/6), 0, \sin(-\pi/6)]^T\right),$$

$$\Delta_{13} = \Delta_1 - \Delta_3 = \left([0, 0, 1]^T - [\cos(-\pi/6), 0, \sin(-\pi/6)]^T\right),$$
$$\Delta_{23} = \Delta_2 - \Delta_3 = \left([\cos(5\pi/6), 0, \sin(-\pi/6)]^T - [\cos(-\pi/6), 0, \sin(-\pi/6)]^T\right).$$

The desired formation trajectory is generated by $(x_d, y_d, z_d)^T = (2\cos(0.3t), 3.1\cos(0.2t) + 0.9\cos(0.15t), 0.2t)^T$. The initial conditions for each quadrotor are $x_{l0} = [2; 0; 0]$, $x_{l1} = [0.8; 0.6; -1.0]$, $x_{l2} = [0; 0.8; 1.0]$, $x_{l3} = [-0.5; 0.8; 0]$. The initial conditions of followers are consistent with the leaders of their respective clusters.

Some necessary parameters are chosen as $\vartheta_f = 0.1, \Gamma_f = 5, \chi_f = 0.01, \theta_f = 0.1, \varrho_f = 0.5$, $\Upsilon_f = 2$ for $f = 1, \ldots, 7$. From Lemma 4.3, by choosing $\zeta = 2$ and $\iota = 0.2$, we can obtain that Q = $0.1409 I_3$, K = -$0.1409 I_3$. Let $\alpha = [0.2, 0.1; 0.1, 0.2]$, $\beta = 1.1$, and $\gamma(0) = 1.1$. The control gains for the distributed formation controller are selected as $k_1 = 3.5, k_2 = 4.2, \alpha_1 = 0.8, \alpha_2 = 0.88$. The physical parameters of the quadrotor aircraft are selected as $m_i = 0.468$, $l = 0.3$, $K_i = 0.1$. To evaluate the robustness of the proposed finite-time controller against perturbations, the following external disturbances are introduced: $d(t) = [0.001 * sin(2t), 0.003 * sin(3t), 0.004 * cos(5t)]^T$.

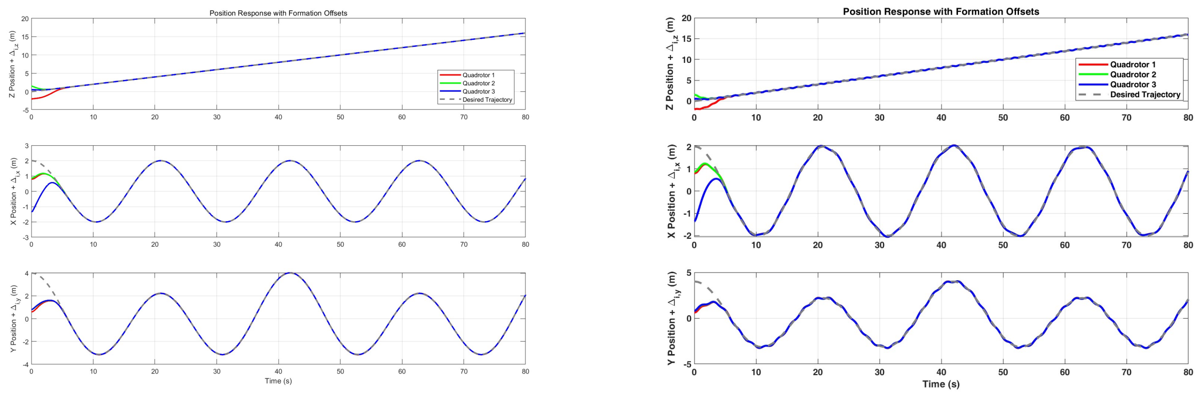

(a) **(b)**

Figure 3. Velocity states and position states of exogenous leader and leaders.

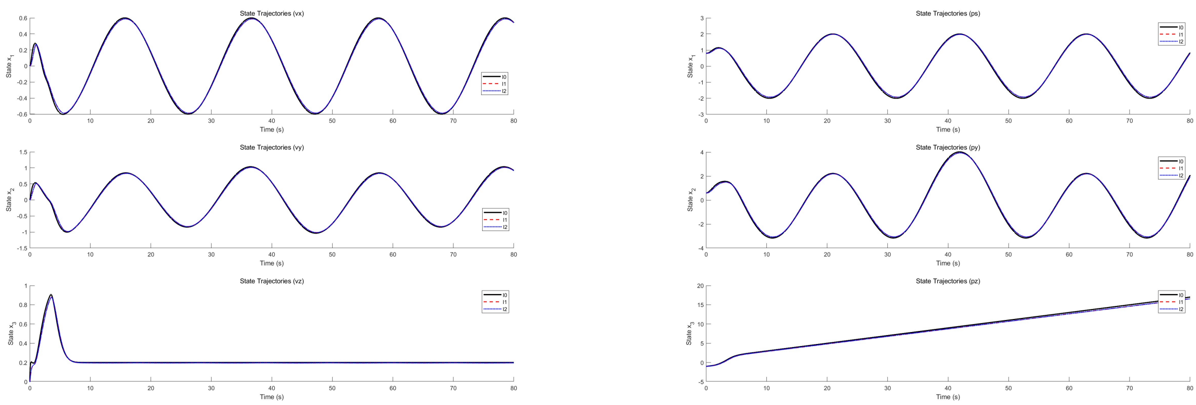

(a) **(b)**

Figure 4. Velocity states and position states of followers and leaders.

The results of numerical simulation are presented in Figures 3–6. Figure 3(a) illustrates the formation tracking performance between the exogenous leader and the cluster leaders in the absence of disturbances, where the leaders effectively track the exogenous leader to establish the formation with observed rapid convergence. Figure 3(b) depicts the tracking performance under external disturbances, demonstrating that the leaders maintain the pre-set formation despite perturbations. Furthermore, Figure 4(a),(b) illustrate the velocity and position states of both followers and leaders in the absence and presence of external disturbances, respectively, indicating that velocity consensus is well-maintained. Figure 5 presents the 3D spatial trajectories of the exogenous leader and the leaders, demonstrating a well-established formation. For comparative analysis, the linear PD controller described in Remark 3.1 was implemented. The results reveal that the proposed finite-time control achieves steady-state convergence in 6.63 s, whereas the PD controller requires 10.03 s. This shows that the proposed strategy yields a significantly faster convergence rate and superior disturbance rejection capabilities.

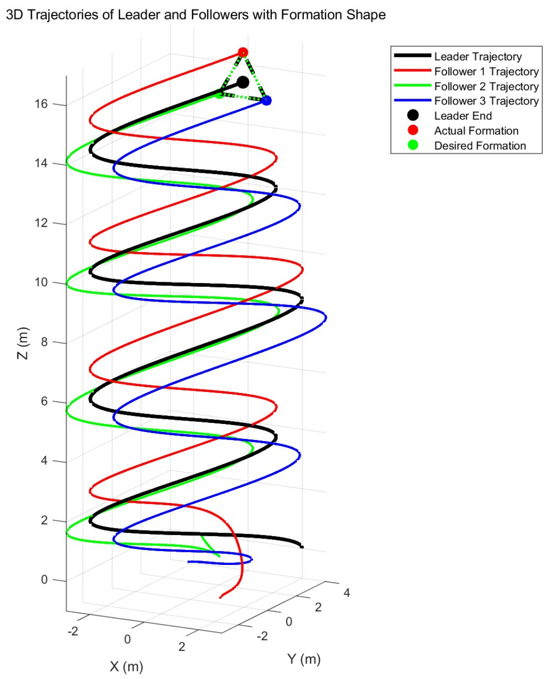

Figure 5. 3D spatial trajectories of the exogenous leader and the leaders.

To rigorously validate the proposed scheme, a high-fidelity simulation platform is used integrating Q Ground Control (QGC), ROS, PX4, and Gazebo. QGC facilitates real-time state monitoring and command transmission, while ROS executes the high-level formation controller to generate attitude setpoints. These references are tracked by the PX4 Autopilot via robust proportional-integral-derivative (PID) loops within the Gazebo physics environment, ensuring a realistic verification of the control performance. The physics engine uses the open dynamics engine solver with a fixed step size of 0.001 s to ensure numerical stability. The state information exchange between agents is handled via the MAVLink protocol, incorporating realistic signal discretization. Figure 6 presents a Gazebo simulation implemented on the high-fidelity PX4 platform, demonstrating that the actual formation closely aligns with theoretical expectations.

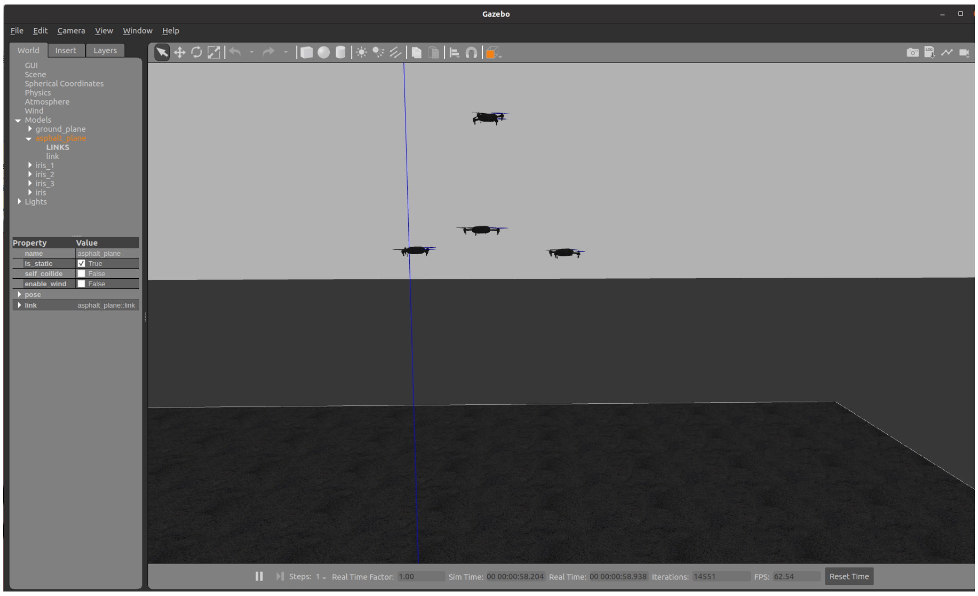

Figure 6. High-fidelity PX4 platform simulation.

6. Conclusions

This work investigates the finite-time formation control problem for a group of quadrotor aircraft subject to dynamic leadership and input saturation. Rigorous theoretical analysis confirms that the proposed distributed control algorithm guarantees finite-time convergence for both the formation pattern and trajectory tracking. The efficacy of this strategy is further corroborated through numerical simulations. However, the impact of complex network constraints, such as communication delays and packet dropouts, remains to be fully addressed. Therefore, future work will focus on enhancing the robustness of the system against external disturbances and distinct unknown communication delays. Additionally, we aim to generalize the proposed framework to a broader class of high-order nonlinear systems and heterogeneous multi-agent systems to expand its applicability.

Use of AI tools declaration

The authors declare they have not used Artificial Intelligence (AI) tools in the creation of this article.

Acknowledgments

This research was supported in part by the National Natural Science Foundation of China under Grants 62173175, 62473226, 62573219, in part by the Natural Science Foundation of Shandong Province under Grants ZR2024MF032 and ZR2024QF039.

Conflict of interest

The authors declare there is no conflicts of interest.

References

1. S. P. Bhat, D. S. Bernstein, Continuous finite-time stabilization of the translational and rotational double integrators, *IEEE Trans. Autom. Control*, **43** (1998), 678–682. https://doi.org/10.1109/9.668834
2. Y. Tang, Terminal sliding mode control for rigid robots, *Automatica*, **34** (1998), 51–56. https://doi.org/10.1016/S0005-1098(97)00174-X
3. S. Yu, X. Yu, B. Shirinzadeh, Z. Man, Continuous finite-time control for robotic manipulators with terminal sliding mode, *Automatica*, **41** (2005), 1957–1964. https://doi.org/10.1016/j.automatica.2005.07.001
4. Y. Feng, X. Yu, F. Han, On nonsingular terminal sliding-mode control of nonlinear systems, *Automatica*, **49** (2013), 1715–1722. https://doi.org/10.1016/j.automatica.2013.01.051
5. J. A. V. Trejo, J. Ponsart, M. Adam-Medina, G. Valencia-Palomo, Fault-tolerant observer-based leader-following consensus control for LPV multi-agent systems using virtual actuators, *Int. J. Syst. Sci.*, **56** (2025), 1816–1833. https://doi.org/10.1080/00207721.2024.2434895
6. Z. Li, Z. Duan, G. Chen, L. Huang, Consensus of multiagent systems and synchronization of complex networks: A unified viewpoint, *IEEE Trans. Circuits Syst. I Regul. Pap.*, **57** (2009), 213–224. https://doi.org/10.1109/TCSI.2009.2013929
7. C. Wang, C. Wen, L. Guo, Adaptive consensus control for nonlinear multiagent systems with unknown control directions and time-varying actuator faults, *IEEE Trans. Autom. Control*, **66** (2021), 4222–4229. https://doi.org/10.1109/TAC.2020.3034209
8. S. N. Campos-Martínez, O. Hernández-González, M. E. Guerrero-Sánchez, G. Valencia-Palomo, B. Targui, F. López-Estrada, Consensus tracking control of multiple unmanned aerial vehicles subject to distinct unknown delays, *Machines*, **12** (2024), 337. https://doi.org/10.3390/machines12050337
9. J. A. V. Trejo, J. C. Ponsart, M. Adam-Medina, G. Valencia-Palomo, D. Theilliol, Distributed observer-based leader-following consensus control for LPV multi-agent systems: Application to multiple VTOL-UAVs formation control, in *2023 International Conference on Unmanned Aircraft Systems*, Warsaw, Poland, (2023), 1316–1323. https://doi.org/10.1109/ICUAS57906.2023.10156012
10. F. Jia, J. Liu, C. L. P. Chen, Z. Wu, Z. Liu, Distributed adaptive consensus for nonlinear multi-agent systems under event-triggered communication using a polynomial approach, *J. Franklin Inst.*, **361** (2024), 106656. https://doi.org/10.1016/j.jfranklin.2024.106656
11. M. Wu, L. B. Wu, G. F. Cui, Event-triggered adaptive control for consensus tracking of multi-agent systems with input saturations and full-state constraints, *J. Math. Anal. Appl.*, **540** (2024), 128572. https://doi.org/10.1016/j.jmaa.2024.128572
12. X. Jiang, R. Jiao, B. Li, X. Zhang, H. Yan, Finite-time consensus of second-order multiagent systems with input saturation via hybrid sliding-mode control, *IEEE Trans. Autom. Sci. Eng.*, **22** (2025), 14623–14632. https://doi.org/10.1109/TASE.2025.3559947
13. H. Ye, M. Li, C. Yang, W. Gui, Finite-time stabilization of the double integrator subject to input saturation and input delay, *IEEE/CAA J. Autom. Sin.*, **5** (2018), 1017–1024. https://doi.org/10.1109/JAS.2018.7511177

14. Z. Zuo, J. Ji, Z. Zhang, Y. Wang, W. Zhang, Consensus of multi-agent systems with asymmetric input saturation over directed graph, *IEEE Trans. Circuits Syst. II Express Briefs*, **70** (2023), 1515–1519. https://doi.org/10.1109/TCSII.2022.3221763
15. J. Wu, L. Huang, Global stabilization of linear systems subject to input saturation and time delays, *J. Franklin Inst.*, **358** (2021), 633–649. https://doi.org/10.1016/j.jfranklin.2020.10.040
16. W. Bai, H. Dong, Z. Zhang, Y. Li, Coordinated time-varying low gain feedback control of high-speed trains under a delayed communication network, *IEEE Trans. Intell. Transp. Syst.*, **23** (2022), 4331–4341. https://doi.org/10.1109/TITS.2020.3043577
17. S. Su, Y. Wei, Z. Lin, Stabilization of discrete-time linear systems with an unknown time-varying delay by switched low-gain feedback, *IEEE Trans. Autom. Control*, **64** (2019), 2069–2076. https://doi.org/10.1109/TAC.2018.2864134
18. B. Zhou, Z. Lin, G. R. Duan, L_∞ and L_2 low-gain feedback: Their properties, characterizations and applications in constrained control, *IEEE Trans. Autom. Control*, **56** (2011), 1030–1045. https://doi.org/10.1109/TAC.2010.2073970
19. Z. Li, X. Liu, W. Ren, L. Xie, Distributed tracking control for linear multiagent systems with a leader of bounded unknown input, *IEEE Trans. Autom. Control*, **58** (2012), 518–523. https://doi.org/10.1109/TAC.2012.2208295
20. Z. Wang, M. Chadli, S. X. Ding, A dynamic event-triggered approach for observer-based formation control of multi-agent systems with designable inter-event time, *Syst. Control Lett.*, **195** (2025), 105970. https://doi.org/10.1016/j.sysconle.2024.105970
21. G. Wang, G. Cheng, W. Wang, L. Xu, Distributed event-based lag consensus formation control for connected and autonomous vehicles, *Chaos, Solitons Fractals*, **202** (2026), 117446. https://doi.org/10.1016/j.chaos.2025.117446
22. O. A. Ángeles-Ramírez, G. Fernández-Anaya, E. G. Hernández-Martínez, J. González-Sierra, M. Ramírez-Neria, Decentralized formation of multi-agent conformable fractional nonlinear robot systems, *Asian J. Control*, **26** (2024), 831–844. https://doi.org/10.1002/asjc.3242
23. C. Li, X. Wang, C. Wei, F. Ren, X. Zong, Z. Zeng, et al., Model-free group formation control of heterogeneous nonlinear multi-agent systems, *Sci. China Inf. Sci.*, **68** (2025), 210209. https://doi.org/10.1007/s11432-025-4587-1
24. M. K. Lu, M. F. Ge, Z. C. Yan, T. F. Ding, Z. W. Liu, An integrated decision-execution framework of cooperative control for multi-agent systems via reinforcement learning, *Syst. Control Lett.*, **193** (2024), 105949. https://doi.org/10.1016/j.sysconle.2024.105949
25. T. F. Ding, S. Gong, M. F. Ge, Z. W. Liu, Z. M. Fang, Performance-guaranteed prescribed-time bipartite consensus of networked Lagrangian agents with bounded inputs and signed digraphs, *J. Franklin Inst.*, **361** (2024), 107217. https://doi.org/10.1016/j.jfranklin.2024.107217
26. N. Yang, J. Li, Distributed robust adaptive learning coordination control for high-order nonlinear multi-agent systems with input saturation, *IEEE Access*, **8** (2020), 9953–9964. https://doi.org/10.1109/ACCESS.2019.2961745
27. S. P. Bhat, D. S. Bernstein, Finite-time stability of continuous autonomous systems, *SIAM J. Control Optim.*, **38** (2000), 751–766. https://doi.org/10.1137/S0363012997321358

28. H. Du, W. Zhu, G. Wen, D. Wu, Finite-time formation control for a group of quadrotor aircraft, *Aerosp. Sci. Technol.*, **69** (2017), 609–616. https://doi.org/10.1016/j.ast.2017.07.012

29. J. Sun, Z. Geng, Y. Lv, Z. Li, Z. Ding, Distributed adaptive consensus disturbance rejection for multi-agent systems on directed graphs, *IEEE Trans. Control Network Syst.*, **5** (2016), 629–639. https://doi.org/10.1109/TCNS.2016.2633804

30. Z. Lin, *Low Gain Feedback*, Springer, London, 1999. https://doi.org/10.1007/978-1-4471-0869-3

31. Y. Lv, Z. Li, Z. Duan, J. Chen, Distributed adaptive output feedback consensus protocols for linear systems on directed graphs with a leader of bounded input, *Automatica*, **74** (2016), 308–314. https://doi.org/10.1016/j.automatica.2016.08.008